

THE REDSHIFT EVOLUTION OF WET, DRY, AND MIXED GALAXY MERGERS FROM CLOSE GALAXY PAIRS IN THE DEEP2 GALAXY REDSHIFT SURVEY

LIHWAI LIN^{1,2}, DAVID R. PATTON³, DAVID C. KOO², KEVIN CASTEELS³, CHRISTOPHER J. CONSELICE⁴, S. M. FABER², JENNIFER LOTZ^{5,6}, CHRISTOPHER N. A. WILLMER⁷, B. C. HSIEH¹, TZIHONG CHIUH⁸, JEFFREY A. NEWMAN⁹, GREGORY S. NOVAK², BENJAMIN J. WEINER⁷, MICHAEL C. COOPER^{7,10}

Draft version November 12, 2018

ABSTRACT

We study the redshift evolution of galaxy pair fractions and merger rates for different types of galaxies using kinematic pairs selected from the DEEP2 Redshift Survey, combined with other surveys at lower redshifts. By parameterizing the evolution of the pair fraction as $(1+z)^m$, we find that the companion rate increases mildly with redshift with $m = 0.41 \pm 0.20$ for all galaxies with $-21 < M_B^e < -19$. Blue galaxies show slightly faster evolution in the blue companion rate with $m = 1.27 \pm 0.35$, while red galaxies have had fewer red companions in the past as evidenced by the negative slope $m = -0.92 \pm 0.59$. The different trends of pair fraction evolution are consistent with the predictions from the observed evolution of galaxy number densities and the two-point correlation function for both the blue cloud and red sequence. For the chosen luminosity range, we find that at low redshift the pair fraction within the red sequence exceeds that of the blue cloud, indicating a higher merger probability among red galaxies compared to that among the blue galaxies. With further assumptions on the merger timescale and the fraction of pairs that will merge, the galaxy major merger rates for $0.1 < z < 1.2$ are estimated to be $\sim 10^{-3} h^3 \text{Mpc}^{-3} \text{Gyr}^{-1}$ with a factor of 2 uncertainty. At $z \sim 1.1$, 68% of mergers are wet, 8% of mergers are dry, and 24% of mergers are mixed, compared to 31% wet mergers, 25% dry mergers, and 44% mixed mergers at $z \sim 0.1$. Wet mergers dominate merging events at $z = 0.2 - 1.2$, but the relative importance of dry and mixed mergers increases over time. The growth of dry merger rates with decreasing redshift is mainly due to the increase in the co-moving number density of red galaxies over time. About 22% to 54% of present-day L^* galaxies have experienced major mergers since $z \sim 1.2$, depending on the definition of major mergers. Moreover, 24% of the red galaxies at the present epoch have had dry mergers with luminosity ratios between 1:4 and 4:1 since $z \sim 1$. Our results also suggest that all three types of mergers play an important role in the growth of the red sequence, assuming that a significant fraction of wet/mixed mergers will also end up as red galaxies. However, the three types of mergers lead to red galaxies in different stellar mass regimes: the wet mergers and/or mixed mergers may be partially responsible for producing red galaxies with intermediate masses while a significant portion of massive red galaxies are assembled through dry mergers at later times.

Subject headings: galaxies:interactions - galaxies:evolution - large-scale structure of universe

1. INTRODUCTION

According to the Λ -dominated Cold Dark Matter (Λ CDM) model, major mergers of galaxies are an important process in the formation of present-day massive galaxies. The merger rate of dark matter halos and galaxies as well as its evolution have now been widely studied with N -body simulations and semi-analytical models (Lacey & Cole 1993; Governato et al. 1999; Gottlöber, Klypin, & Kravtsov 2001; Khochfar & Burkert 2001; Maller et al 2006; Berrier et al. 2006; Fakhouri & Ma 2007; Guo & White 2008; Mateus 2008). Measuring the frequency of galaxy close pairs and

galaxy merger rates thus provides powerful constraints on theories of galaxy formation and evolution. The galaxy merger fraction is often parameterized by a power law of the form $(1+z)^m$. Observational studies of galaxy merger rates using both close pairs and morphological approaches within the last decade have found a diverse range of m values from $m \sim 0$ to ~ 4 (Zepf & Koo 1989; Burkey, Keel, & Windhorst 1994; Carlberg et al. 1994; Yee & Ellingson 1995; Woods, Fahlman, & Richer 1995; Neuschaefer et al. 1997; Patton et al. 1997; Carlberg et al. 2000; Le Fèvre et al. 2000; Patton et al. 2002; Conselice et al. 2003; Bundy et al. 2004; Lin et al. 2004; Cassata et al. 2005; Conselice 2006; Bell et al. 2006b; Lotz et al. 2008; Kampeczyk et al. 2007; Kartaltepe et al. 2007). This discrepancy may arise from the different sample selections across different redshift ranges, as well as from different procedures used to correct for the sample incompleteness. The relatively mild evolution of observed galaxy mergers found in the literature (Carlberg et al. 2000; Bundy et al. 2004; Lin et al. 2004; Lotz et al. 2008) seems to be in contradiction to the rapid increase of halo merger rates with redshift predicted in N -body numerical simulations where $m \sim 3$ (Governato et al. 1999; Gottlöber, Klypin, & Kravtsov 2001). Nevertheless, such comparison may not be adequate since the latter were focused on the merger histories of distinct halos which host one or multiple galaxies. On the other hand, the mergers of

¹ Institute of Astronomy & Astrophysics, Academia Sinica, Taipei 106, Taiwan; Email: lihwailin@asiaa.sinica.edu.tw

² UCO/Lick Observatory, Department of Astronomy and Astrophysics, University of California, Santa Cruz, CA 95064

³ Department of Physics and Astronomy, Trent University, 1600 West Bank Drive, Peterborough, ON K9J 7B8 Canada

⁴ School of Physics and Astronomy, University of Nottingham, Nottingham, NG72RD UK

⁵ National Optical Astronomy Observatory, 950 N. Cherry Ave., Tucson, AZ 85719

⁶ Leo Goldberg Fellow

⁷ Steward Observatory, University of Arizona, 933 N. Cherry Avenue, Tucson, AZ 85721 USA

⁸ Department of Physics, National Taiwan University, Taipei, Taiwan

⁹ Physics and Astronomy Dept., University of Pittsburgh, Pittsburgh, PA, 15620

¹⁰ Spitzer Fellow

subhalos in N -body simulations offer a better analogy to the observed galaxy mergers. In a recent study using N -body simulations, Berrier et al. (2006) find that the companion rate of subhalos increases mildly with redshift out to $z \sim 1$, consistent with the data presented in Lin et al. (2004).

Despite the successful agreement between pair counts of observed galaxies and subhalos in simulations, it is not yet clear whether low or mild evolution of the pair fraction and merger rate still holds for different types of galaxies. The intrinsic color distribution of galaxies has been shown to be bi-modal since $z \sim 1$ (Bell et al. 2004; Faber et al. 2007). It is thus expected that the effects of interactions and mergers between various types of galaxies on their final products can be different. For example, 'wet mergers' (mergers between two gas-rich galaxies) can trigger additional star formation (Barton et al. 2000; Lambas et al. 2003; Nikolic, Cullen, & Alexander 2004; Woods, Geller, & Barton 2006; Lin et al. 2007; Bridge et al. 2007; Barton et al. 2007), cause quasar activity (Hopkins et al. 2006) and transform disk galaxies into ellipticals (Toomre & Toomre 1972). On the other hand, the so-called 'dry mergers' (mergers between two gas-poor galaxies) may not involve dramatic changes in the star formation rate, but can play an important role in the stellar mass growth of massive red galaxies at the current epoch (Tran et al. 2005; van Dokkum 2005; Bell et al. 2006a; Faber et al. 2007; McIntosh et al. 2007; Khochfar & Burkert 2003, 2005; Naab, Khochfar, & Burkert 2006; Cattaneo et al. 2008). In addition, the relative fraction of mixed pairs versus separation might yield clues on the effectiveness of a red galaxy to shut down the star formation even of other galaxies in its neighborhood. Quantifying the merger rates of galaxies between different types is therefore an important step towards understanding how present day massive galaxies are built up.

While recently there have been several efforts attempting to estimate the merger rates of certain categories, they were mainly focused on red galaxies (van Dokkum 2005; Bell et al. 2006a; Masjedi et al. 2006; Lotz et al. 2008; Masjedi, Hogg, & Blanton 2007). Yet no direct observational measurement of the relative abundances of wet, dry, and mixed mergers has been provided. despite that they have been explored in recent theoretical studies (Khochfar & Burkert 2003; Ciotti et al. 2007). In this work, we investigate the evolution of the pair fractions for different types of galaxies and obtain the relative fraction of major merger rates among various types of mergers for the first time. We classify close galaxy pairs into three different categories (blue-blue pairs; red-red pairs; mixed pairs) based on galaxy colors. As a first approximation, blue galaxies are gas-rich while red galaxies are gas-poor. We therefore calculate the merger rates of wet mergers, dry mergers, and mixed mergers using the number statistics from blue-blue pairs, red-red pairs and mixed pairs. There is however possible contamination of red gaseous and blue gas-poor galaxies in our analysis. Recent studies of galaxy morphologies have suggested that about 20% of red galaxies appear to be either edge-on disks or dusty galaxies and hence are likely to be gas-rich (Weiner et al. 2005). On the other hand, there also exist blue spheroidals that could be gas-poor, although these are relatively rare objects (Cassata et al. 2007). Since both cases of contamination discussed above affect only a minority of the red sequence and blue clouds respectively, classifying different types of mergers based on their colors should be a good approximation. The pair sample is constructed based on their rest-frame B -band luminosity L_B as often used in the literature. While the stel-

lar mass range of red and blue galaxies selected with fixed L_B could be different, L_B is shown to be a good tracer of dynamical mass for a wide range of Hubble types (Kannappan & Wei 2008). Therefore, in this work we select major-merger candidates based on the ratio of L_B regardless of the color difference.

The galaxy sample at $0.45 < z < 1.2$ is taken from the DEEP2 Redshift Survey (Davis et al. 2003, 2007) and Team Keck Redshift Survey in GOODS-N (Wirth et al. 2004). We also supplement our low redshift sample ($z < 0.45$) using the SSRS2 survey (da Costa et al. 1998), Millennium Galaxy Catalog (hereafter MGC, Liske et al. 2003; Driver et al. 2005; Allen et al. 2006) and CNOC2 Redshift Survey (Yee et al. 2000). The combined samples yield the largest number of kinematic pairs out to $z \sim 1.2$ to date and enable study, for the first time, of galaxy merger rates for wet mergers, dry mergers and mixed mergers as a function of redshift.

In §2, we describe the selection of close pairs. In §3, we present our results on the pair fractions for blue and red galaxies, as well as the derived merger rates for different merger categories. A discussion is given in §4, followed by our conclusions in §5. Throughout this paper we adopt the following cosmology: $H_0 = 100h \text{ km s}^{-1} \text{ Mpc}^{-1}$, $\Omega_m = 0.3$ and $\Omega_\Lambda = 0.7$. The Hubble constant $h = 0.7$ is adopted when calculating rest-frame magnitudes. Unless indicated otherwise, magnitudes are given in the AB system.

2. DATA, SAMPLE SELECTIONS, AND METHODS

Close pairs are potential progenitors of merging galaxies and hence present an opportunity to study the different types of mergers before coalescence takes place. Thanks to the high spectral resolution of DEEP2 ($\sim 30 \text{ km s}^{-1}$) and TKRS ($\sim 60 \text{ km s}^{-1}$), we are able to select kinematic pairs at $0.45 < z < 1.2$, which require accurate spectroscopic redshifts of both pair components in order to reduce the contamination by interlopers. Three other redshifts surveys including galaxies at lower redshift ($z < 0.5$) - SSRS2, MGC, and CNOC2 - are also added to our sample.

2.1. K -correction and Sample selection

The rest-frame B -band magnitudes (M_B) and $U - B$ colors for DEEP2 galaxies at $0.45 < z < 0.9$ are derived in a similar way to that in Willmer et al. (2006). For galaxies with $0.9 < z < 1.2$, the rest-frame $U - B$ color is computed using the observed $R - z_{\text{mega}}$ color, where z_{mega} is the z -band magnitude obtained from CFHT/Megacam observations for DEEP2 Fields in 2004 and 2005 (Lin et al. 2008, in preparation). The K -corrections for the TKRS sample are described in Weiner et al. (2006).

We started from a sample of galaxies with $-21 < M_B^e < -19$, where M_B^e is the evolution-corrected absolute magnitude, defined as $M_B + Qz$. The values of Q are found to be close to 1.3 up to $z \sim 1$ for either blue or red galaxies (Faber et al. 2007). Throughout this paper, we therefore adopt $Q = 1.3$ to ensure that galaxies within the same range of the luminosity function are being selected. Kinematic close pairs are then identified such that their projected separations satisfy $10 h^{-1} \text{ kpc} \leq r_p \leq r_{\text{max}}$ (physical length) and rest frame relative velocities Δv less than 500 km s^{-1} (Patton et al. 2000; Lin et al. 2004).

Galaxies are further divided into the blue cloud and red sequence using the rest-frame magnitude dependent cut for DEEP2 and TKRS (in AB magnitudes):

$$U - B = -0.032(M_B + 21.62) + 1.035. \quad (1)$$

Fig. 1 shows the rest-frame color-magnitude diagram for one of the DEEP2 fields (EGS) in three redshift bins. The solid lines denote the above color cut to separate the blue and red galaxies. The vertical dotted lines in each panel indicate the approximate bright and faint limit of M_B corresponding to $-21 < M_B^e < -19$. It can be seen that the red galaxies are not complete in the highest redshift bin (*bottom left*) due to the $R = 24.1$ cut in the DEEP2 sample. We will discuss how to deal with such incompleteness in §3.1.

For the low redshift samples, simple rest-frame color cuts $g-r = 0.65$ (in AB) and $B-R = 1.02$ (in AB) are applied to MGC and CNOC2 respectively. In Fig. 2, we plot the relation between the rest-frame $g-r$ and $U-B$ (*top*) and between the rest-frame $B-R$ and $U-B$ (*bottom*) using the synthesized colors from templates of Kinney et al. (1996). As shown in Fig. 2, there is a fairly good correlation between these colors. Therefore the $g-r$ cut for MGC and the $B-R$ cut for CNOC2 can still provide good correspondence of blue and red galaxies at low-redshifts to the DEEP2 sample. Fig. 3 shows the color versus the evolution-corrected B -band magnitude for MGC and CNOC2 (*top and bottom, respectively*), with the two dotted lines corresponding to the $-21 < M_B^e < -19$ cut. Blue-blue pairs, red-red pairs, and mixed pairs (hereafter b-b, r-r, and mixed pairs respectively) are classified according to the color combination of the pairs. In total, we have 218 b-b pairs, 122 r-r pairs, and 166 mixed pairs with $10 h^{-1} \text{kpc} \leq r_p \leq 50 h^{-1} \text{kpc}$ and $\Delta v \leq 500 \text{ km s}^{-1}$ from combined samples.

2.2. The Spectroscopic Selection Function and Weights

To measure the incompleteness of the DEEP2 survey and hence the selection function, we compared the sample with successful redshifts to all objects in the photometric catalog that satisfy the limiting magnitude and any photometric redshift cut. The selection function is expected to depend on an unknown and complex interplay among observables and intrinsic properties of objects. With data too limited to undertake multi-dimensional investigations of the selection function, we make the simplifying assumption that the selection function is separable in the different observed variables (Yee, Ellingson, & Carlberg 1996). By assuming that fluxes are the only observables correlated to the other observables of galaxies, we restrict the definition of the selection function to be

$$S = S_m \overline{S_c} \overline{S_{SB}} \overline{S_{xy}} = S_m(R) \frac{S_c(B-R, R-I, R)}{S_m(R)} \frac{S_{SB}(\mu_R, R)}{S_m(R)} \frac{S_{xy}}{S_m(R)}, \quad (2)$$

where S_m is the magnitude selection function, S_c is the apparent color selection function, S_{SB} is the surface brightness selection function and S_{xy} represents the geometric (local density) selection function. $\overline{S_c}$, $\overline{S_{SB}}$, and $\overline{S_{xy}}$ are all normalized to the magnitude selection function, S_m . The spectroscopic weight w for each galaxy is thus $1/S$, which is derived from its apparent R mag, $B-R$ and $R-I$ colors, R band surface brightness, and local galaxy density.

The magnitude selection function $S_m(R)$ (the left panel of Fig. 4) of each galaxy is computed as the ratio of the number of galaxies with good redshift qualities to the total number of galaxies in the target catalog in both cases considering a magnitude bin of ± 0.25 mag centered on the magnitude of the galaxy. The color selection function $S_c(B-R, R-I, R)$ (the middle panel of Fig. 4) is computed by counting galaxies within $\pm 0.25 R$ magnitude over a $B-R$ and $R-I$ color range of ± 0.25 mag. Similarly, the surface brightness selection

function (the right panel of Fig. 4) is performed within ± 0.25 mag in μ_R and ± 0.25 mag in R . The geometric selection function $S_{xy}(xy, R)$ is similar to magnitude selection function but has a localized effect. We take the ratio between the number of galaxies with good quality redshifts and the total number in the targeted catalog in an area of radius 120" within a $\pm 0.25 R$ -magnitude range. The left panel of Fig. 5 shows the distribution of S_{xy} . Finally we use Equation 2 to compute the total selection function S , which leads to the spectroscopic weight for each galaxy in DEEP2 as $w = 1/S$.

Besides the selection function for each individual galaxy, we also investigate the selection dependence on pair separation using analogous procedures adopted by Patton et al. (2002). In principle, the target selection is unlikely to place slits on close pairs simultaneously since the slit orientations constrained to be less than ± 30 degs from the slit mask orientation. In addition, we are not able to put slits on objects that are very close to each other because their separate spectra will overlap. The suppression of close pairs, however, is not a severe problem in DEEP2 because each field has been observed with two masks. To quantify this effect, we measure the angular separation of all pairs in the redshift catalog (z - z pairs) and in the target catalog (p - p pairs) respectively and then count the number of pairs (N_{zz} and N_{pp}) within each angular separation bin. While counting the pairs in the redshift catalog, each component of a pair is weighted by a geometric selection function $S_{xy}(xy)$ to exclude the effect due to the variance in the local sampling rate. The angular selection function S_θ is computed as the ratio between the weighted N_{zz} and N_{pp} . The angular weight, w_θ , for each galaxy is hence $1/S_\theta$ (see the right panel of Fig. 5).

We repeat the above analysis for the TKRS sample except that the ACS $B-V$ and $V-i$ colors are used when calculating the color selection function. The selection function and weights for SRS2, MGC, and CNOC2 samples are computed in the same manner as described in Patton et al. (2000, 2002).

3. RESULTS

3.1. The Pair Fraction for the Blue Cloud, the Red Sequence and Full Galaxy Sample

We first compute the pair fraction N_c , defined as the average number of companions per galaxy:

$$N_c = \frac{\sum_{i=1}^{N_{tot}} \sum_j w_j w(\theta)_{ij}}{N_{tot}}, \quad (3)$$

where N_{tot} is the total number of galaxies within the chosen absolute magnitude range, w_j is the spectroscopic weight for the j th companion belonging to the i th galaxy, and $w(\theta)_{ij}$ is the angular selection weight for each pair as described in §2.2. While the blue galaxy sample is volume-limited for the adopted magnitude range $-21 < M_B^e < -19$, because of the $R = 24.1$ cut in the DEEP2 sample, lower luminosity red galaxies beyond $z \sim 1$ are not contained in the sample. To estimate the missing fraction of galaxies, we extrapolated the derived red luminosity function of DEEP2 (Willmer et al. 2006) and calculated the expected total number of galaxies between $-21 < M_B + Qz < -19$ at $z \sim 1.1$. These predicted numbers are then compared to the predicted number of galaxies between $-21 < M_B + Qz < M_{limit}(24.1)$, where $M_{limit}(24.1)$ represents the faint limit imposed by the apparent $R=24.1$ cut used by DEEP2. The latter comprise $\sim 42\%$ from which we estimate that about 58% of the galaxies could be missing in the sample. Therefore we apply a correction factor of 2.4 for each red

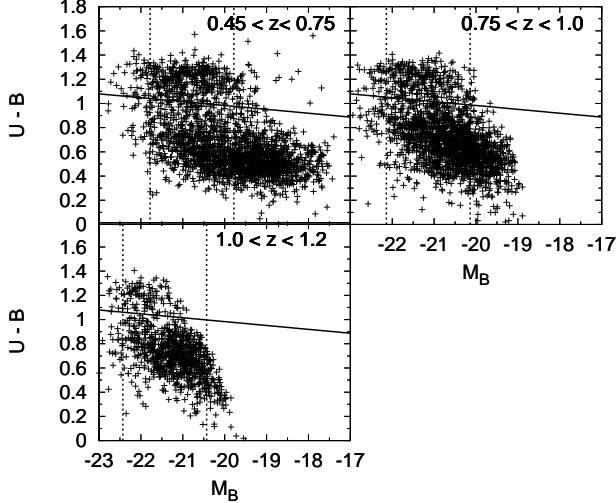


FIG. 1.— Restframe $U-B$ vs. absolute B -band magnitude for galaxies in one of the DEEP2 fields (EGS). The solid lines denote the color cut (see Equation 1) to separate the blue and red galaxy populations. The vertical dotted lines in each panel indicate the approximate bright and faint limit of absolute B magnitude (M_B) at the mean redshift of each redshift range used to pick up pair samples.

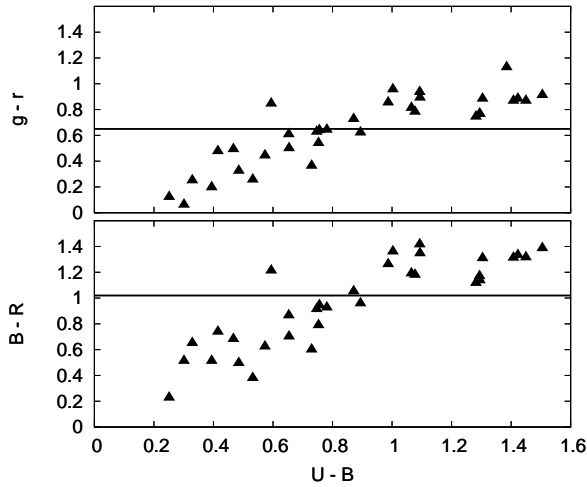


FIG. 2.— Synthesized $g-r$ vs. $U-B$ color and $B-R$ vs. $U-B$ color from galaxy templates of Kinney et al. (1996). It can be seen that both the rest-frame $g-r$ and $B-R$ colors correlate well with the rest-frame $U-B$ color. The solid lines denote the color thresholds adopted in our work to separate the blue and red galaxy populations for MGC and CNOC2 samples respectively.

companion at $z > 1$ in addition to the usual spectroscopic and angular separation corrections.

Fig. 6 (see also Table 1) shows N_c versus redshift with $r_{max} = 30 h^{-1}$ kpc, $50 h^{-1}$ kpc, and $100 h^{-1}$ kpc (from top to bottom, respectively) from four types of measurement: a) N_c from all pairs regardless of colors; b) the average number of blue companions per blue galaxy N_c^b ; c) the average number of red companions per red galaxy N_c^r ; d) the average number of companions of galaxies with opposite colors to that of the primary galaxies N_c^m . Types b) and c) are equivalent to the pair fraction within the blue cloud and red sequence respectively. If the pair fraction is fitted by $N_c(0)(1+z)^m$ with both $N_c(0)$ and m as free parameters, we find that m varies among different color samples (Table 2). When considering all colors together, we find a minor amount of evolution with a power-law index of $m = 0.41 \pm 0.20$ for the case of $r_{max} = 30 h^{-1}$ kpc

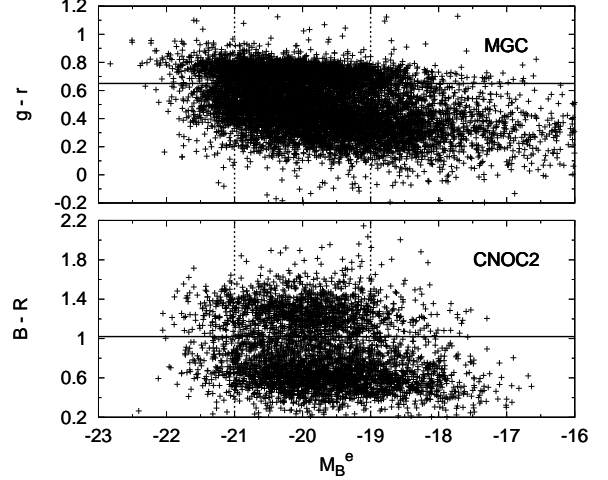


FIG. 3.— Upper: rest-frame $g-r$ vs. evolution-corrected absolute B -band magnitude (M_B^e) diagram. Lower panel: rest-frame $B-R$ vs. evolution-corrected absolute B -band magnitude (M_B^e). The solid lines denote the color thresholds adopted in our work to separate the blue and red galaxy populations. The vertical dotted lines in each panel indicate the bright and faint limit of M_B^e used to select samples for pair studies.

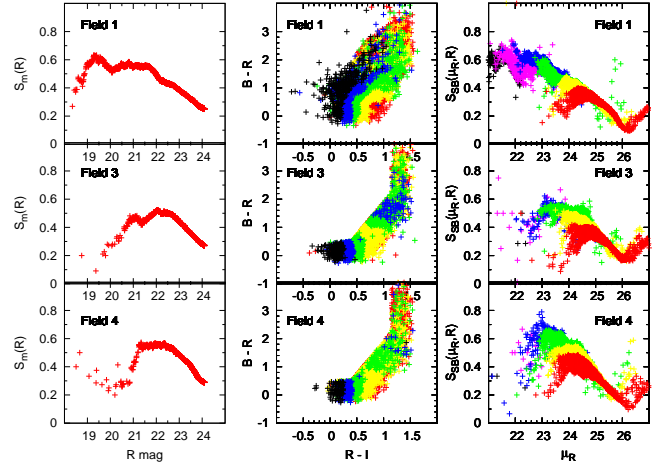


FIG. 4.— (1) Left: the apparent R -band magnitude selection $S_m(R)$ as a function of the apparent R -band magnitude. The peak completeness is about 55% \sim 60%. (2) Middle: the apparent color selection function $S_c(B-R, R-I, R)$ as a function of the apparent color $B-R$ and $R-I$ for DEEP2. The colors correspond to various ranges of the selection function (red is for $S_c > 0.5$; yellow is for $0.4 < S_c < 0.5$; green is for $0.3 < S_c < 0.4$; blue is for $0.2 < S_c < 0.3$; black is for $S_c < 0.2$). (3) Right: the apparent R -band surface brightness selection function $S_{SB}(\mu_R, R)$ as a function of the apparent R -band surface brightness for DEEP2. The colors correspond to the apparent R -band magnitude (red is for $23.5 < R < 24.1$; yellow is for $23 < S_c < 23.5$; green is for $22 < R < 23$; blue is for $21 < R < 22$; magenta is for $20 < R < 21$; black is for $R < 20$).

, and $m = 0.41 \pm 0.14$ for the case of $r_{max} = 50 h^{-1}$ kpc. These results are consistent with the value 0.51 ± 0.28 given in Lin et al. (2004), which used a sample 7 times smaller. Blue galaxies, however, have stronger evolution $m = 1.27 \pm 0.35$, meaning that the probability of blue galaxies having a blue companion is higher at higher redshift. Red galaxies, on the other hand, have higher chance of being found in r-r pairs at lower redshifts than at high redshifts, as indicated by the negative power index ($m = -0.92 \pm 0.59$). Finally, N_c^m , which measures the mixed pair fraction, is also found to decrease with increasing redshifts ($m = -1.52 \pm 0.42$). Except for the mixed pairs, there is very weak dependence of m on the chosen r_{max} , suggesting that our derived m is not strongly affected

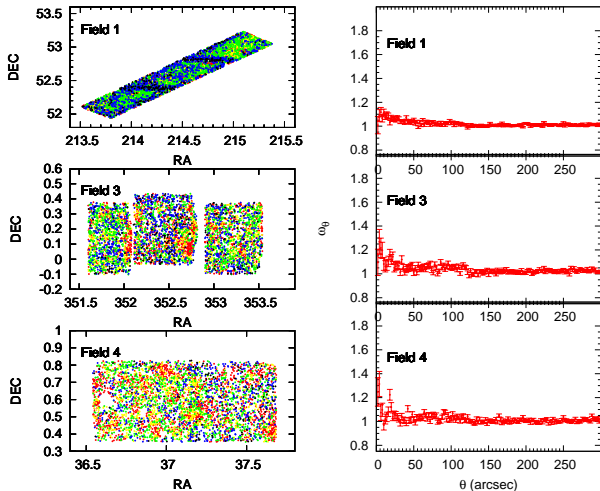


FIG. 5.— Left: The spatial distribution of the geometric selection function for DEEP2 Fields 1, 3, and 4. The colors correspond to various ranges of the selection function (red is for $S_c > 0.5$; yellow is for $0.4 < S_c < 0.5$; green is for $0.3 < S_c < 0.4$; blue is for $0.2 < S_c < 0.3$; black is for $S_c < 0.2$). Right: The angular weights (ω_θ) as a function of angular separation (θ) of pairs.

by the incomplete sampling rate at small scales. On the other hand, the significant change of m for mixed pairs when varying r_{max} may indicate a change in the environment that hosts mixed pairs over time.

The evolutionary trends of blue and red galaxies can be understood as follows: the pair fraction is proportional to the galaxy number density times the integral at small scales of the real space 2-point correlation function. The galaxy correlation function is normally approximated by a power law $\xi = (r/r_0)^{-\gamma}$ at distances ranging from 0.1 to several Mpc. Under the assumption that the clustering strength at small scales follows the same power law, the pair fraction inside a physical radius R can be related to the correlation function as

$$f_{pair} \sim n_g \int_0^{R/a} \xi 4\pi r^2 dr \propto n_g \frac{\gamma_0^\gamma}{3-\gamma} R^{3-\gamma} (1+z)^{3-\gamma}, \quad (4)$$

where a is the expansion factor, R is the maximum separation of close pairs in physical length, and n_g is the comoving galaxy number density. The study of galaxy clustering of DEEP2 galaxies suggests that there has been little evolution in γ for either blue or red galaxies since $z \sim 1$, and r_0 increases slightly, by 10% and 15% for blue and red galaxies respectively, from $z \sim 1$ to $z \sim 0$ (Coil et al. 2008). Adopting $\gamma = 1.64$ (2.06) for blue (red) galaxies at $z = 1$ (Coil et al. 2008), and accounting for the increase in number density of blue (red) galaxies by a factor of 1 (2) since $z = 1$ (Faber et al. 2007), we obtain $m = 1.14$ (-0.48) for blue (red) galaxies by comparing the pair fraction at $z = 1$ and $z = 0$ using Equation 4. These values of m are fully consistent with what we have found for kinematic pairs of both blue and red galaxies, indicating that the pair fraction evolution is a natural consequence of evolution of galaxy number density and galaxy clustering. While consistency with the overall number density and correlation function studies is encouraging, the close pairs we use here directly probe what is really happening on small scales (ie. rather than an inward extrapolation of the correlation function).

3.2. The Major Merger Rates of Wet Mergers, Dry Mergers, and Mixed Mergers

Here we define the galaxy major merger rates as the number of merger events involving at least one galaxy within $-21 < M_B^e < -19$ to merge with another galaxy with luminosity ratio between 4:1 and 1:4 per unit volume per gigayear. This quantity can be derived from the pair fraction together with the known galaxy number density and the assumption about the timescale of being pairs before final mergers. It is worth noting, however, the pair fraction in §3.1 is computed using pairs drawn from within a luminosity range of 2 mag. Some true companions may fall outside the absolute magnitude range of our sample, while some selected companions have luminosity ratios outside the range of 4:1 to 1:4. To account for both of these effects, we use the following equation to convert the pair fraction for the case of $r_{max} = 30 h^{-1} \text{kpc}$ into merger rates (Lin et al. 2004):

$$N_{mg} = (0.5 + G) \times n_g(z) C_{mg} N_c(z) T_{mg}^{-1}, \quad (5)$$

where T_{mg} is the timescale for close pairs to merge, C_{mg} denotes the fraction of galaxies in close pairs that will merge within T_{mg} , $n_g(z)$ is the comoving number density of galaxies, and G is the correction factor that accounts for the selection effect of companions due to the restricted luminosity range. The factor of 0.5 converts the number of merging galaxies into the number of merger events (i.e., on average, two close companions correspond to one galaxy pair and hence one merger). The smallest separation pairs with $r_{max} = 30 h^{-1} \text{kpc}$ are the best tracers of future mergers, and hence our calculations below of merger rates are based on the pair statistics from pairs with $r_{max} = 30 h^{-1} \text{kpc}$. We adopt a crude value of $T_{mg} = 0.5$ Gyr, as suggested by major merger simulations (Conselice 2006; Lotz et al. 2008b) and $C = 0.6$, by estimating the fraction of pairs that are closer than $30 h^{-1} \text{kpc}$ in real 3-D space among those selected by $10 h^{-1} \text{kpc} \leq r_p \leq r_{max} h^{-1} \text{kpc}$ and $\Delta v < 500 \text{ km s}^{-1}$. It is worth noting that the uncertainty of T_{mg} is at least a factor of 2. Here we make a simple assumption that T_{mg} is the same for all types of mergers. The motivation behind this is that the B -band light is a good tracer of dynamical mass (Kannappan & Wei 2008) and hence the merger timescales should be approximately similar for red, blue-blue, and mixed pairs when selected with a fixed M_B range at a given redshift. The correction factor G for wet and dry mergers is defined as

$$1 + G = \frac{\int_{M_B^{min}(z)}^{M_B^{max}(z)} n(M, z) dM \int_{M-1.5}^{M+1.5} n(M', z) dM'}{(\int_{M_B^{min}(z)}^{M_B^{max}(z)} n(M, z) dM)^2}, \quad (6)$$

where $M_B^{min}(z) = -21 - Qz$, and $M_B^{max}(z) = -19 - Qz$ in our case. Here $n(M, z)$ is the galaxy number density for galaxies with magnitude M at redshift z . The numerator in Equation 6 gives the integrated number density of the secondary sample used to search for companions with a luminosity ratio between 4:1 and 1:4 relative to the primary galaxies, weighted by the number density of primary galaxies within $-21 < M_B^e < -19$ ¹¹. The denominator gives the integrated number density of companions with $-21 < M_B^e < -19$ weighted by that of the primary galaxies within the same luminosity range. This calculation assumes that the number of companions per galaxy traces the number density of galaxies as measured by the luminosity function, and assumes that there is no luminosity-dependent clustering.

¹¹ The primary galaxy can be either the bright one or the less luminous one in pairs

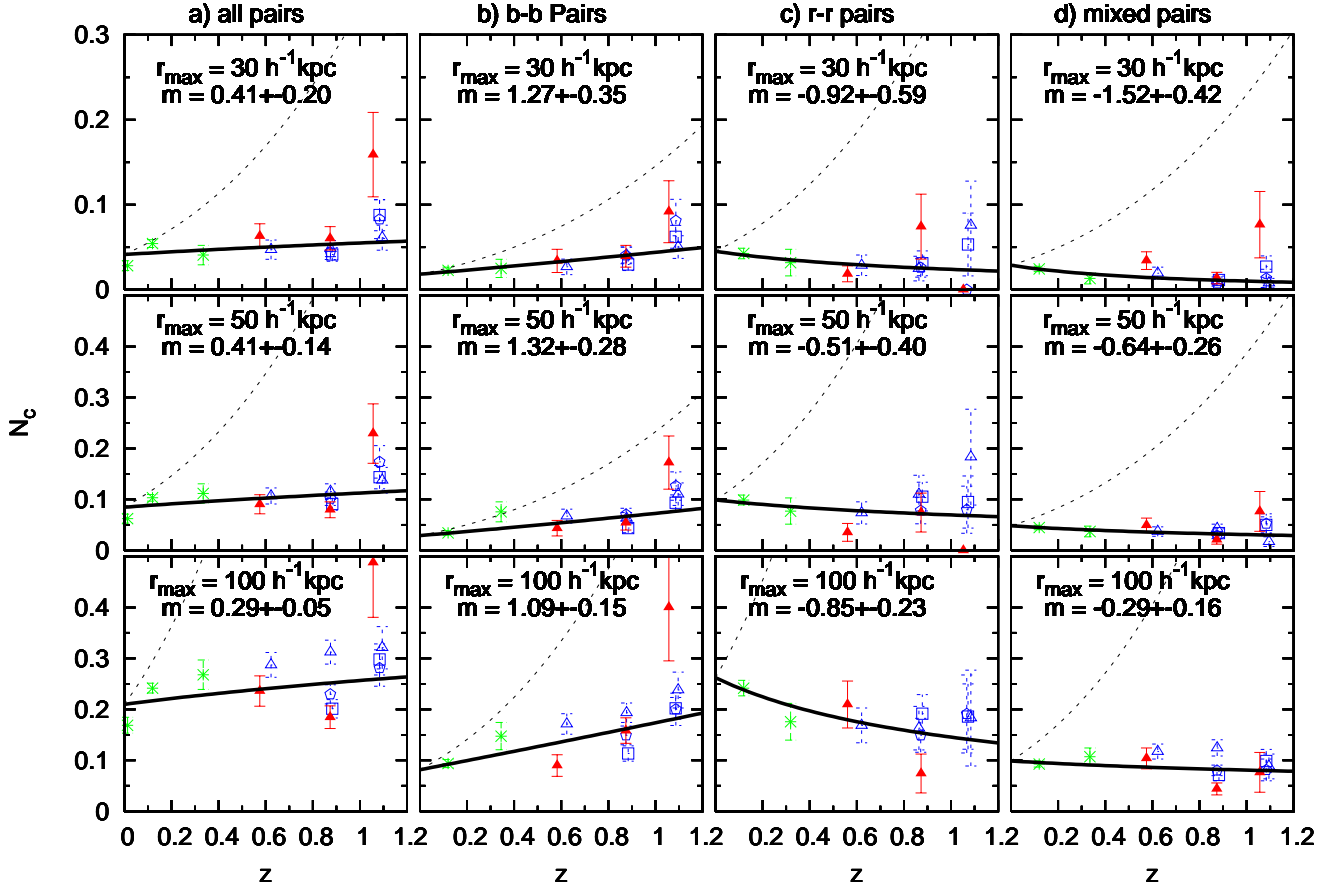


FIG. 6.— The pair fraction as a function of redshift for different types of close pairs using $r_{\max}=30 h^{-1}$ kpc (top panel), $50 h^{-1}$ kpc (middle panel), and $100 h^{-1}$ kpc (bottom panel). From left to right: all pairs, b-b pairs, r-r pairs, and mixed pairs. Colors represent data points from different surveys; green for the SSRS2 ($\bar{z} \sim 0.01$), MGC ($\bar{z} \sim 0.12$), and CNOC2 ($\bar{z} \sim 0.34$); blue for the DEEP2 Fields 1 (blue triangles), 3 (squares), and 4 (pentagons); red is for TKRS. The points lying on the X-axis represent the fields where no pairs have been found; they are not included when calculating the fits. The best fits are shown as solid lines while the dotted lines represent the $m = 3$ curves. Different types of pairs evolve differently as a function of redshift denoted by the value of evolution power m shown on each plot. The error bars shown in the plot and used for fitting are calculated by bootstrapping.

For mixed mergers, the above equation is modified into

$$\begin{aligned}
 1 + G = & \left[\int_{M_B^{\min}(z)}^{M_B^{\max}(z)} n_1(M, z) dM \int_{M-1.5}^{M+1.5} n_2(M', z) dM' \right. \\
 & + \left. \int_{M_B^{\min}(z)}^{M_B^{\max}(z)} n_2(M, z) dM \int_{M-1.5}^{M+1.5} n_1(M', z) dM' \right] \\
 / & \left[\int_{M_B^{\min}(z)}^{M_B^{\max}(z)} n_1(M, z) dM \int_{M_B^{\min}(z)}^{M_B^{\max}(z)} n_2(M', z) dM' \right. \\
 & + \left. \int_{M_B^{\min}(z)}^{M_B^{\max}(z)} n_2(M, z) dM \int_{M_B^{\min}(z)}^{M_B^{\max}(z)} n_1(M', z) dM' \right], \quad (7)
 \end{aligned}$$

where n_1 and n_2 denote the galaxy number density for blue and red galaxies respectively. We use Equation 6 and Equation 7 to compute G by adopting galaxy luminosity functions of blue and red galaxies in the literature (see Table 5 of Faber et al. 2007). The value of G is found to range from 0.4 to 1.3, depending on the galaxy type and the redshift range.

Fig. 7 displays the major merger rates as function of redshift for three types of mergers (wet mergers, dry mergers, and mixed mergers). When considering all types of mergers together, it shows that the absolute merger rate remains fairly constant at $1 \times 10^{-3} h^3 \text{Mpc}^{-3} \text{Gyr}^{-1}$ for $0.1 < z < 1.2$ while the average wet merger rate is about $7 \times 10^{-4} h^3 \text{Mpc}^{-3} \text{Gyr}^{-1}$

over the same redshift range. On the other hand, dry mergers and mixed mergers are found to increase over time. The increase rate of dry merger rates is faster than that of the red pair fraction due to the increase in comoving number density of red galaxies towards lower redshift. It is worth noting that the uncertainty of the absolute merger rates quoted above is at least a factor of 2 due to the uncertainty in T_{mg} .

Fig. 8 shows the relative fraction of different mergers in a given redshift bin. At $z > 0.2$, wet mergers dominate the merger events while dry mergers contribute by a much lesser degree. However, at $z = 0.1$, the relative proportions are more similar. The ratio between wet mergers, dry mergers, and mixed mergers is 9:1:3 at $z \sim 1.1$ and 6:5:9 at $z \sim 0.1$, indicating that the role of dry and mixed mergers becomes increasingly important towards lower redshifts. We also compare our results with the theoretical predictions of the relative fraction of mergers for different morphological types (Khochfar & Burkert 2003). These predictions are based on semi-analytical galaxy formation models (Kauffmann et al. 1999; Springel et al. 2001) and merger tree techniques described in Somerville & Kolatt (1999). More details of the models used by Khochfar & Burkert (2003) can be found in Khochfar & Silk (2006). The three colored lines in Fig. 8 represent the model predictions of the fraction of mergers between early-type galaxies (E-E), late-type galaxies (Sp-Sp),

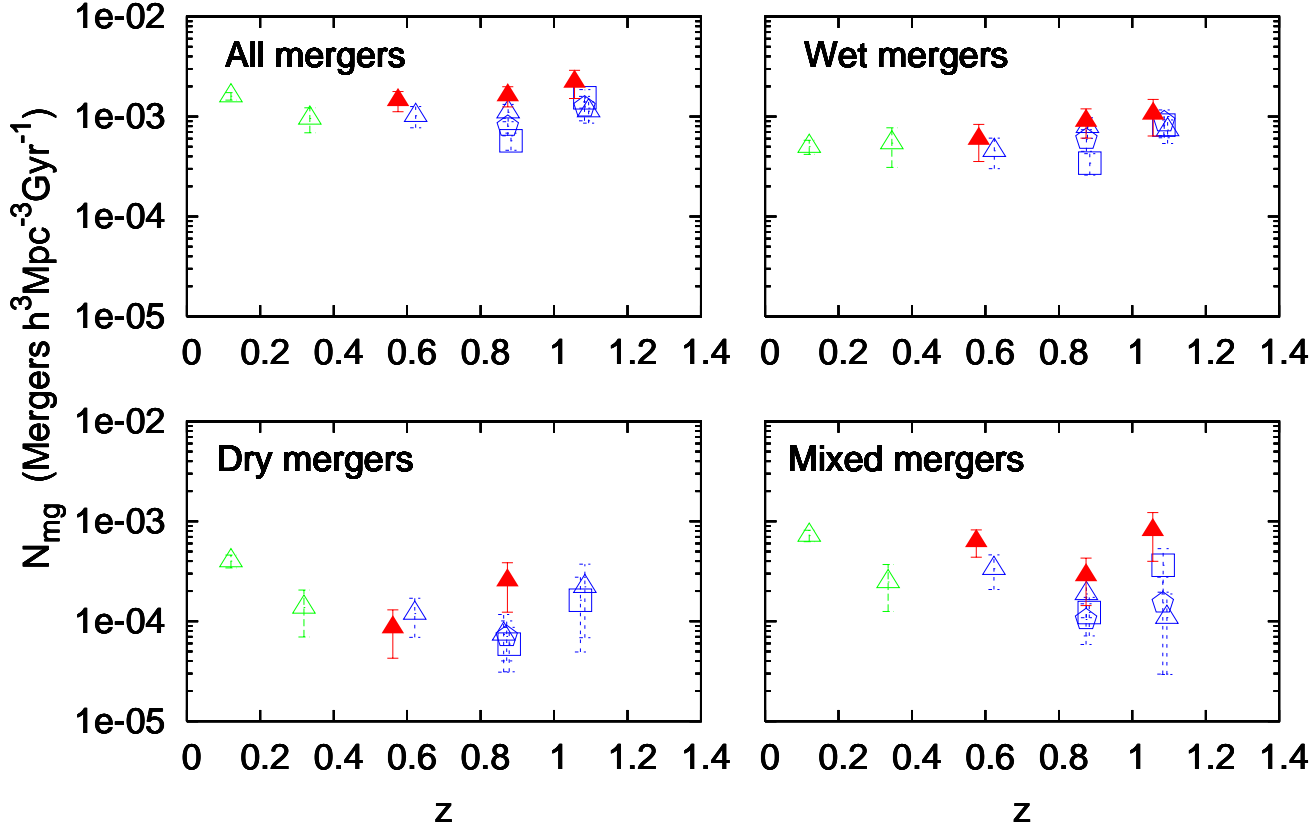


FIG. 7.— Comoving volume major merger rate as a function of redshift for the various types of mergers as indicated in the plots. Different symbols represent data from different survey fields as described in Fig. 6. The errors shown here represent the uncertainty coming from the pair counts in our samples, and do not include the uncertainties of T_{mg} and C_{mg} .

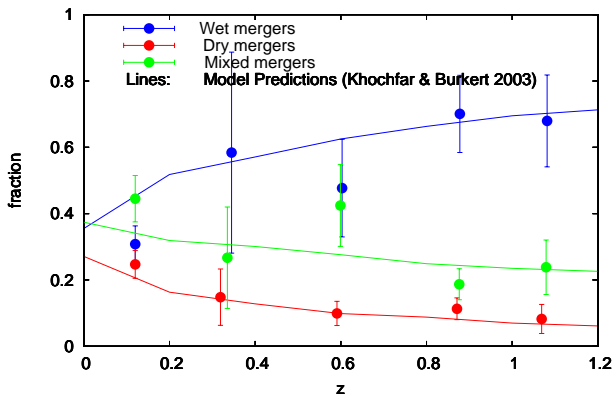


FIG. 8.— Fraction of major mergers for wet (blue symbols), dry (red symbols), and mixed mergers (green symbols) as a function of redshift. The data points represent results from the DEEP2, TKRS, CNOC2 and MGC surveys. The three color lines show the semi-analytical predictions of Sp-Sp, E-E, and E-Sp mergers by Khochfar & Burkert (2003) but for a field-like environment, corresponding to a dark matter halo of mass $M_0 \sim 10^{13} M_\odot$. The data and the model prediction are in good agreement, both showing an increasing fraction of dry (E-E) and mixed (E-Sp) mergers with decreasing redshift.

and mixed mergers (E-Sp) for a field-like environment, corresponding to a dark matter halo of mass $M_0 \sim 10^{13} M_\odot$. Our observational result is in good agreement with the model pre-

dictions by Khochfar & Burkert (2003), both showing an increasing fraction of dry and mixed mergers with decreasing redshift since $z \sim 1$.

4. DISCUSSION

From the analysis of spectroscopic close pairs, we find that the pair fraction and its evolution depend on the colors of galaxies. By parameterizing the pair fraction $N_c \propto (1+z)^m$, m is found to be 0.41 ± 0.2 for the full sample of $0.4L^* < L < 2.5L^*$ galaxies regardless of the companion's color, consistent with the previous result by Lin et al. (2004). It is also in good agreement with the theoretical predictions using pairs of subhalos (Berrier et al. 2006). Blue galaxies have slightly faster evolution in the blue companion rate (N_c^b) as $m \sim 1.3$ while red galaxies possess inverse evolution with $m \sim -0.9$ in the red companion rate (N_c^r).

Our analysis of N_c , N_c^b , N_c^r , or N_c^m rules out rapid redshift evolution for $m > 3$ at a 4-sigma level. This evolutionary trend in the pair fraction can be explained within the context of the observed evolution of the two-point correlation function (Coil et al. 2008) and the galaxy number density (Faber et al. 2007). After converting the pair fraction into galaxy merger rates with the assumed merging fraction in pairs and the merger timescale, we find that the absolute merger rate is about $1 \times 10^{-3} h^3 \text{Mpc}^{-3} \text{Gyr}^{-1}$ (with a factor of 2 uncertainty) for $0.1 < z < 1.2$. Adopting $h = 0.7$, our estimate is in good agreement with the merger rate $2 - 4 \times 10^{-4}$

$\text{Gyr}^{-1} \text{Mpc}^{-3}$ obtained by Lotz et al. (2008) based on morphological approaches. At $z \sim 1.1$, 68% of mergers are wet, 8% of mergers are dry, and 24% of mergers are mixed, compared to 31% wet mergers, 25% dry mergers, and 44% mixed mergers at $z \sim 0.1$. Wet mergers dominate merging events at $z = 0.2 - 1.2$, but the relative importance of dry and mixed mergers increases over time. The good agreement between our observed fraction of various types of mergers and the predicted results in Khochfar & Burkert (2003) using semi-analytical models supports the importance of the merging hypothesis within the framework of hierarchical structure formation. In the following sections we discuss several implications of our results.

4.1. Mild Evolution or Fast Evolution ?

The mild evolution of pair fractions and merger rates from $z \sim 1$ to 0 is consistent with several previous studies from either pair counts or morphologies (Carlberg et al. 2000; Lin et al. 2004; Lotz et al. 2008), but disagrees with other recent works (Le Fèvre et al. 2000; Conselice et al. 2003; Cassata et al. 2005; Kampczyk et al. 2007; Kartaltepe et al. 2007) which claim much higher evolution rates. However, as discussed in Patton et al. (2002) and Lin et al. (2004), the pair fraction or merger fraction is a function of galaxy luminosity, hence its evolution depends on how the samples are defined. Moreover, photometric pairs suffer from the contamination by interlopers, although the spectroscopic pairs may be biased since no spectroscopic survey is complete. Therefore applying careful projection and completeness corrections in a consistent way across the entire redshift range is crucial to pin down the true pair/merger fraction. Lotz et al. (2008) also point out that part of the evidence for rapid evolution in the literature comes from the adopted low pair or merger fraction at $z \sim 0$. In this work, we select galaxies within a luminosity range such that they evolve in the same way as the L^* galaxies out to $z = 1.2$, and apply spectroscopic corrections based on the characteristics of each sample to account for the various spectroscopic selection effects.

The low-redshift pair fraction at $z \sim 0.1$ obtained here using the MGC sample with $10 h^{-1} \text{kpc} \leq r_p \leq 30 h^{-1} \text{kpc}$ and $\Delta v \leq 500 \text{ km s}^{-1}$ is 5.4%, which is close to the value of 4.1% determined independently by De Propris et al. (2007) using same data set but with slightly different pair selection criteria ($r_p \leq 20 h^{-1} \text{kpc}$; $\Delta v \leq 500 \text{ km s}^{-1}$; $-21 \leq M_B - 5 \log h \leq -18$). Both of these results are higher than the pair fraction of the SDSS sample reported by Kartaltepe et al. (2007) and (Bell et al. 2006b). Future works calibrating the merger fraction at low redshifts (Patton & Atfield 2008) will help to disentangle the issue of different evolutionary trends (also see the discussion in Lotz et al. 2008).

4.2. The Accumulated Merger Fraction since $z \sim 1.2$

To determine the accumulated effect of major mergers on galaxies at the present epoch, we calculate the fraction of present day galaxies that have undergone major mergers since $z \sim 1.2$. We consider two cases here: one has mergers among galaxies within $-21 < M_B^e < -19$ (i.e., the luminosity of both pair components is within $0.4L^* < L < 2.5L^*$); the other is for galaxies with $-21 < M_B^e < -19$ that merge with companions with luminosity ratios ranging between 4:1 and 1:4. In the first case, we follow Equation (32) in Patton et al. (2000):

$$f_{rem} = 1 - \prod_{j=1}^N \frac{1 - C_{mg} N_c(z_j)}{1 - 0.5 C_{mg} N_c(z_j)}, \quad (8)$$

where f_{rem} is the remnant fraction, $C_{mg} N_c$ gives the fraction of galaxies that will undergo mergers during the time interval T_{mg} , and z_j corresponds to a look-back time of $t = jT_{mg}$. Adopting $C_{mg} = 0.6$ as used in §3.2, and $N_c(z)$ from the fit of the data for the case of $r_{max} = 30 h^{-1} \text{kpc}$, our result implies that 22% of today's galaxies with $0.4L^* < L < 2.5L^*$ have experienced mergers with galaxies within the same luminosity range since $z \sim 1.2$.

In the second case which is a better probe of the major merger rate, Equation 8 needs to be modified as:

$$f_{rem} = 1 - \prod_{j=1}^N \frac{1 - (1+G)C_{mg} N_c(z_j)}{1 - 0.5 C_{mg} N_c(z_j)}, \quad (9)$$

where the term $(1+G)$ accounts for the missed companions (see §3.2). Since the factor G is approximately 1 at all redshifts, we conclude that about 54% of $0.4L^* < L < 2.5L^*$ galaxies have undergone a major merger since $z \sim 1.2$, but this depends sensitively on the assumed merger timescale. Both estimates above of the remnant fraction are about 2-6 times greater than that reported in Lin et al. (2004). The major cause of this difference can be traced to the different definitions of major mergers as well as the different choice of pair separations when calculating the remnant fraction.¹²

4.3. The Roles of Dry Mergers in the Formation of Massive Galaxies

Previous works have suggested that dry mergers are likely responsible for the growth of massive galaxies on the red sequence (Bell et al. 2004; Faber et al. 2007), because of the lack of blue galaxies massive enough to migrate from the blue cloud to the red sequence. Moreover, there is observational evidence showing the nonnegligible amount of dry mergers occurring in the past 8 Gyr (van Dokkum 2005; Bell et al. 2006a, White et al. 2007, although see Masjedi et al. 2006; Scarlata et al. 2007), as well as evidence from theoretical expectations (Khochfar & Burkert 2003; Naab, Khochfar, & Burkert 2006; Cattaneo et al. 2008). We now discuss the implication of our merger studies on this topic. We have shown that at a given luminosity range, the merger events are always dominated by wet mergers, followed by mixed mergers, and then dry mergers in terms of the event rates over the redshift range $0.2 < z < 1.2$. This is mainly because the number density of blue galaxies dominates the total galaxy population in the luminosity range we consider. However, given the fact that the pair fraction and merger rate also depend on the clustering properties of galaxies in addition to the galaxy number density, the probability of red galaxies having a red companion N_c^r turns out to be comparable to the blue companion rate for blue galaxies N_c^b at $z < 1.2$. At $z < 0.4$, N_c^r becomes even greater than N_c^b as shown in Fig. 6 and Table 5. That is to say, the probability of mergers within the red sequence is greater than that within the blue cloud at low redshifts.

We can compare our results to previous attempts at measuring the dry merger frequency. Our derived N_c^r average over

¹² Lin et al. (2004) calculated the remnant fraction by using pairs with $r_{max} = 20 h^{-1} \text{kpc}$ and by requiring both merger components to have $-21 < M_B^e < -19$.

$0.1 < z < 0.7$ is similar to the fraction of dry-merger candidates $\sim 3\%$ found by Bell et al. (2006a) from the GEMS survey. In addition, our fitted dry pair fraction at $z \sim 0$ is about 0.045 (see Table 2), which is also in broad agreement with the companion fraction (~ 0.06) within the red sequence estimated by van Dokkum (2005) using nearby galaxy samples. On the other hand, Masjedi et al. (2006) found very small merger rates for luminous red galaxies, on the order of $0.6 \times 10^4 \text{ Gyr}^{-1} \text{ Gpc}^{-3}$ from the SDSS Luminous Red Galaxy sample (LRG). Their finding is about 23 times lower than our estimates of dry merger rates at $z \sim 0.1$ and 7 times lower than ours at $z \sim 0.3$ ¹³. The major discrepancy can be attributed to the different luminosity ranges being sampled: their choice of faint-end magnitude is brighter than typical L^* galaxies by almost 2 mag while ours is fainter than L^* by 1 mag. Since the luminosity function of red galaxies shows a strong decline towards the bright end, we expect that mergers occurring among luminous red galaxies should be much lower than that among less-luminous ones. This effect is also found by Patton et al. (2002) and Lin et al. (2004).

In order to assess how much dry mergers with luminosity ratios less than 4:1 may contribute to the growth of massive red galaxies, we compute the following quantities, $\langle N_{mg}^{dry} \rangle > T_z / n_g^r(0)$, where $\langle N_{mg}^{dry} \rangle$ is the average dry merger rate over $0 < z < 1$, T_z is the cosmic time since $z = 1$, and n_g^r is the number density of red galaxies within a 2 mag bin centered on L^* at $z = 0$. Taking $\langle N_{mg}^{dry} \rangle$ as $2 \times 10^{-4} h^3 \text{ Mpc}^{-1} \text{ Gyr}^{-1}$, T_z as 8 Gyr, and $n_g^r(0) \sim 6.7 \times 10^{-3} h^3 \text{ Mpc}^{-1}$, we find that about 24% of present red galaxies have experienced dry mergers. Our result is slightly lower than the 35% found by van Dokkum (2005), mainly because they have assumed a constant dry merger rate over time while we find a decreasing rate of dry mergers with increasing redshift.

4.4. The Role of Mixed and Wet Mergers vs. Dry Mergers

The contribution of mixed mergers and wet mergers to the formation of red galaxies is less straightforward to constrain given the difficulty in handling how often and how soon the mixed and wet mergers transform the merger remnant into a red sequence galaxy. Under the extreme assumption that both mixed mergers and wet mergers lead to the formation of red galaxies immediately, the fraction of present day red galaxies that have experienced mixed and wet mergers is roughly 36% and 71% respectively. These values are certainly over-estimated since not necessarily all remnants of mixed or wet mergers end up in the red sequence. We note that at a fixed luminosity, the stellar mass of red galaxies is systematically higher than that of blue galaxies (see Equation 1 of Lin et al. 2007); in other words, the stellar mass of the progenitors of dry mergers is larger than that of wet mergers or mixed mergers in our sample since we select the pairs based on the luminosity cut in both the blue cloud and red sequence. For example, the typical stellar mass of our selected blue galaxies is $\sim 2 \times 10^{10} M_\odot$ and that of our red galaxies is $\sim 10^{11} M_\odot$. Hence, the merger remnant of these three types of mergers being considered in our sample will likely end up as red galaxies in different stellar mass regimes. A plausible scenario is that the star formation is quenched after the process of wet mergers and/or mixed mergers, resulting in the formation of some portion of the red galaxies with intermediate masses.

The massive red galaxies are then built up through dry mergers between galaxies with intermediate masses at a later time since our results suggest that dry-mergers play an increasing role at lower redshifts.

5. CONCLUSION

Combining the DEEP2, TKRS, MGC, CNOC2, and SSRS2 catalogs, we study the redshift evolution of the pair fraction and major merger rates of wet, dry, and mixed mergers for galaxies with $-21 < M_B^e < -19$ out to $z \sim 1.2$. The merger candidates are identified as close pairs based on their projected separation on the sky and relative line-of-sight velocities. Wet, dry, and mixed mergers are classified according to the colors of the individual components in close pairs. Our results can be summarized as follows:

1. Parameterizing the evolution of the pair fraction as $(1 + z)^m$, we find that $m = 0.41 \pm 0.20$ for the full sample, consistent with the low value of m as found by Lin et al. (2004).

2. The values of m depend on the color combination in close pairs. Blue galaxies show slightly faster evolution in the blue companion rate with $m = 1.27 \pm 0.35$ while red galaxies have had fewer red companions in the past as evidenced by the negative slope $m = -0.92 \pm 0.59$. On the other hand, $m = -1.52 \pm 0.42$ for mixed pairs. The different trends of the pair fraction evolution are consistent with the predictions from the observed evolution of galaxy number densities and the two-point correlation function for both the blue cloud and red sequence.

3. For the chosen luminosity range, we find that at low redshift ($z < 0.4$) the pair fraction within the red sequence is greater than that of the blue cloud, indicating a higher merger probability within the red sequence compared to that within the blue cloud.

4. With further assumptions on the merger timescale and the fraction of pairs that will merge, the galaxy major merger rates for $0.1 < z < 1.2$ are estimated to be $\sim 10^{-3} h^3 \text{ Mpc}^{-3} \text{ Gyr}^{-1}$ (with the uncertainty about a factor of 2), dominated by wet mergers (gas-rich mergers) until very recently. There were more wet merger events than dry or mixed mergers because of the higher number density of blue galaxies for the chosen luminosity cut. However, the fraction of mergers which are dry or mixed increases over time, from 8% and 24% at $z \sim 1$ to 25% and 44% at $z = 0$ respectively. The growth of dry merger rates with decreasing redshift is mainly due to the rise in the co-moving number density of red galaxies with time. Our results on the fraction of mergers of different types are in good agreement with theoretical predictions by Khochfar & Burkert (2003) based on semi-analytical models.

5. About 22% to 54% of present-day L^* galaxies have experienced major mergers since $z \sim 1.2$, depending on the definition of major mergers. Moreover, 24% of the red galaxies at the present epoch have had dry mergers with luminosity ratio less than 4:1 since $z \sim 1$.

6. Given the B -band luminosity cut, the blue and red galaxies in our sample possess different stellar masses: the typical stellar mass of red galaxies in our sample is about 5 times greater than that of the blue galaxies. By assuming that a significant fraction of wet/mixed mergers will end up as red galaxies as well as dry mergers, our results suggest that the three types of mergers lead to red galaxies in different stellar mass regimes: the wet mergers and/or mixed mergers may be partially responsible for producing red galaxies with intermediate masses while dry mergers in our sample produce a significant portion of massive red galaxies at low redshift.

¹³ Note that their merger rates are quoted using the unit $\text{Gpc}^{-3} \text{ Gyr}^{-1}$ while our results in Table 5 are in $h^3 \text{ Mpc}^{-3} \text{ Gyr}^{-1}$. We adopt $h = 0.7$ when doing comparisons.

We have demonstrated that the redshift evolution of pair fractions and merger rates depend on galaxy types, owing to the color dependence of the evolution in the galaxy number density and clustering. In terms of the absolute number of events, wet mergers dominate merger events at $0.2 < z < 1.2$. However, dry and mixed mergers become more important over time, in particular at very low redshifts ($z < 0.2$). Our findings support the late growth of massive red galaxies through dry mergers as concluded by van Dokkum (2005) and Bell et al. (2006a). Moreover, our results also suggest that wet and mixed mergers are responsible for producing red-sequence galaxies in lower stellar mass regimes. More observational and theoretical studies on the effects of the three types of mergers on the star formation in the merger remnants will help us to constrain better the role of galaxy mergers in forming red-sequence galaxies. One uncertainty that can affect the relative importance of the three types of mergers is that we have adopted a constant merger timescale for all types of mergers in our analysis. This approach is based on the assumption that the B -band light is a good tracer of dynamical mass (Kannappan & Wei 2008) and hence the merger timescale should be comparable in different types of pairs selected by the same M_B cut. Future works to pin down the merger timescale more precisely will be valuable in determining the relative importance among wet, dry, and mixed mergers.

We thank the referee for a very thorough and helpful report. This work was supported by NSF grants AST00-

71198, AST05-07428 and AST05-07483, an NSERC Discovery Grant to D. R. P, and an NSC grant NSC95-2112-M-002-013 to T. Chiueh. We thank Olivier Le Fèvre, Alison Coil, Arjun Dey, Youjun Lu, and Sheila Kannappan for useful discussions; S. Khochfar and A. Burkert for providing data from their previous theoretical works and for helpful comments; the Taiwan CosPA project for accessing CFHT Observing time; the staff of CFHT for conducting MegaCam Observations and image pre-processing; Laurent Domisse of the Terapix team for data reduction and stacking; and David Gilbank and Alex Conley for providing defringing program to process the MegaCam images. This work is based in part on data products produced at the TERAPIX data center located at the Institut d'Astrophysique de Paris.

The DEEP2 Redshift Survey has been made possible through the dedicated efforts of the DEIMOS instrument team at UC Santa Cruz and support of the staff at Keck Observatory.

The Millennium Galaxy Catalogue consists of imaging data from the Isaac Newton Telescope and spectroscopic data from the Anglo Australian Telescope, the ANU 2.3m, the ESO New Technology Telescope, the Telescopio Nazionale Galileo and the Gemini North Telescope. The survey has been supported through grants from the Particle Physics and Astronomy Research Council (UK) and the Australian Research Council (AUS). The MGC data and data products are publicly available from <http://www.eso.org/~jliske/mgc/> or on request from J. Liske or S.P. Driver.

We close with thanks to the Hawaiian people for use of their sacred mountain.

REFERENCES

- Allen, P. D., Driver, S. P., Graham, A. W., Cameron, E., Liske, J., & De Propris, R. 2006, MNRAS, 371, 2
- Barton, E. J., Geller, M. J., & Kenyon S. J. 2000, ApJ, 530, 660
- Barton, E. J., Arnold, J. A., Zentner, A. R., Bullock, J. S., & Wechsler, R. H. 2007, ApJ, 671, 1538
- Bell, E. F. et al. 2004, ApJ, 608, 752
- Bell, E. F. et al. 2006a, ApJ, 640, 241
- Bell, E. F., Phleps, S., Somerville, R. S., Wolf, C., Borch, A., & Meisenheimer, K. 2006b, ApJ, 652, 270
- Berrier, J. C., Bullock, J. S., Barton, E. J., Guenther, H. D., Zentner, A. R., & Wechsler, R. H. 2006, ApJ, 652, 56
- Bridge, C. R., et al. 2007, ApJ, 659, 931
- Bundy, K., Fukugita, M., Ellis, R. S., Kodama, T., & Conselice, C. J. 2004, ApJ, 601, L123
- Burkey, J. M., Keel, W. C., & Windhorst, R. A. 1994, ApJ, 429, L13
- Carlberg, R. G., Pritchett, C. J., & Infante, L. 1994, ApJ, 435, 540
- Carlberg, R. G., et al. 2000, ApJ, 532, L1
- Cassata, P., et al. 2005, MNRAS, 357, 903
- Cassata, P., et al. 2007, ApJS, 172, 270
- Cattaneo, A., Dekel, A., Faber, S. M., & Guiderdoni, B. 2008, preprint (arXiv:0801.1673)
- Ciotti, L., Lanzoni, B., & Volonteri, M. 2007, ApJ, 658, 65
- Coil, A. L., et al. 2008, 672, 153
- Conselice, C. J., Bershady, M. A., Dickinson, M., & Papovitch, C. 2003, AJ, 126, 1183
- Conselice, C. J. 2006, ApJ, 638, 686
- da Costa, L. N., et al. 1998, AJ, 116, 1
- Davis, M., et al. 2003, SPIE, 4834, 161
- Davis, M., et al. 2007, ApJ, 660, L1
- De Propris, R. et al. 2007, ApJ, 666, 212
- Driver, S. P., Liske, J. N., Cross, J. G., De Propris, R. and Allen, P.D. 2005, MNRAS, 360, 81
- Faber, S. M., et al. 2007, ApJ, 665, 265
- Fakhouri, O., & Ma, C.-P. 2007, preprint (arXiv:0710.4567)
- Gottlöber, S., Klypin, A., & Kravtsov, A. V. 2001, ApJ, 546, 223
- Governato, F., Gardner, J. P., Stadel, J., Quinn, T., & Lake, G. 1999, AJ, 117, 1651
- Guo, Q., & White, S. D. M. 2008, MNRAS, 384, 2
- Hopkins, P. F., Hernquist, L., Cox, T. J., Di Matteo, T., Robertson, B., & Springel, V. 2006, ApJS, 163, 1
- Kampeczyk, P., et al. 2007, ApJS, 172, 329
- Kannappan, S., & Wei, L. 2008, In Proceedings of "The Evolution of Galaxies through the Neutral Hydrogen Window", eds. R. Minchin and E. Momjian, AIP Conference Proceedings, in press
- Kartaltepe, J. S., et al. 2007, ApJS, 172, 320
- Kauffmann, G., Colberg, J. M., Diaferio, A., & White, S. D. M. 1999, MNRAS, 307, 529
- Khochfar, S., & Burkert, A. 2001, ApJ, 561, 517
- Khochfar, S., & Burkert, A. 2003, ApJ, 597, L117
- Khochfar, S., & Burkert, A. 2005, MNRAS, 359, 1379
- Khochfar, S., & Silk, J. 2006, MNRAS, 370, 902
- Kinney, A. L., Calzetti, D., Bohlin, R. C., McQuade, K., Storchi-Bergmann, T., & Schmitt, H. R. 1996, ApJ, 467, 38
- Lacey, C., & Cole, S. 1993, MNRAS, 262, 627
- Lambas, D. G., Tissera, P. B., Alonso, M. S., & Coldwell, G. 2003, MNRAS, 346, 1189
- Le Fèvre, O., et al. 2000, MNRAS, 311, 565
- Lin, L. et al. 2004, ApJ, 617, L9
- Lin, L. et al. 2007, ApJ, 660, L51
- Liske, J., Lemon, D.J., Driver, S.P., Cross, N.J.G., and Couch, W.J. 2003, MNRAS, 344, 307
- Lotz, J. M., et al. 2008, ApJ, 672, 177
- Lotz, J. M., Jonsson, P., Cox, T. J., & Primack, J. R. 2008, preprint (arXiv:0805.1246)
- Maller, A. H., Katz, N., Kereš, D., Davé, R., & Weinberg, D. H. 2006, ApJ, 647, 763
- Masjedi, M., et al. 2006, ApJ, 644, 54
- Masjedi, M., Hogg, D., & Blanton, M. 2007, preprint (arXiv:0708.3240)
- Mateus, A. 2008, preprint (arXiv:0802.2720)
- McIntosh, Daniel H., Guo, Y., Hertzberg, J., Katz, N., Mo, H. J., van den Bosch, Frank C., & Yang, X. 2007, preprint (arXiv:0710.2157)
- Naab, T., Khochfar, S., & Burkert, A. 2006, ApJ, 636, L81
- Neuschaefer, L. W., Im, M., Ratnatunga, K. U., Griffiths, R. E., & Casertano, S. 1997, ApJ, 480, 59
- Nikolic, B., Cullen, H., & Alexander, P. 2004, MNRAS, 355, 874

TABLE 1. PAIR STATISTICS USING $r_{max} = 30 h^{-1} \text{kpc}$ AND COMOVING VOLUME MERGER RATES

Sample	\bar{z}	N_c	N_c^b	N_c^r	N_c^m	N_{mg}	N_{mg}^{wet}	N_{mg}^{dry}	N_{mg}^{mix}
DEEP2 Field 1	0.623	0.047±0.011	0.027±0.009	0.029±0.012	0.019±0.007	1.02E-03	4.55E-04	1.20E-04	3.35E-04
(EGS)	0.875	0.048±0.010	0.041±0.009	0.025±0.014	0.010±0.004	1.10E-03	7.88E-04	7.39E-05	1.88E-04
...	1.094	0.061±0.015	0.050±0.013	0.076±0.052	0.008±0.006	1.13E-03	7.31E-04	2.21E-04	1.09E-04
DEEP2 Field 3	0.883	0.041±0.008	0.030±0.007	0.031±0.015	0.011±0.005	5.71E-04	3.42E-04	5.91E-05	1.22E-04
...	1.084	0.088±0.018	0.062±0.014	0.053±0.037	0.027±0.013	1.54E-03	8.22E-04	1.63E-04	3.64E-04
DEEP2 Field 4	0.874	0.044±0.009	0.040±0.010	0.026±0.011	0.007±0.003	8.03E-04	5.93E-04	7.04E-05	1.04E-04
...	1.083	0.083±0.023	0.081±0.025	0.000±0.000	0.013±0.011	1.25E-03	8.88E-04	0.000E+00	1.53E-04
TKRS	0.575	0.063±0.014	0.034±0.014	0.019±0.009	0.034±0.010	1.45E-03	5.94E-04	8.64E-05	6.29E-04
...	0.874	0.060±0.014	0.039±0.013	0.074±0.038	0.014±0.007	1.62E-03	9.00E-04	2.54E-04	2.86E-04
...	1.056	0.159±0.050	0.092±0.037	0.000±0.000	0.076±0.039	2.21E-03	1.06E-03	0.000E+00	8.11E-04
SSRS2	0.014	0.028±0.006
MGC	0.120	0.054±0.005	0.023±0.004	0.043±0.006	0.024±0.003	1.60E-03	4.98E-04	4.00E-04	7.20E-04
CNOC2	0.335	0.041±0.011	0.025±0.011	0.032±0.016	0.013±0.007	9.55E-04	5.41E-04	1.37E-04	2.47E-04

NOTE. — Here N_c is the companion rate per galaxy; N_c^b is the blue companion rate per blue galaxy; N_c^r denotes the red companion rate per red galaxy; N_c^m gives the average number of companions with colors opposite that of the primary galaxy. N_{mg} , N_{mg}^{wet} , N_{mg}^{dry} , N_{mg}^{mix} are the comoving merger rate for total mergers, wet mergers, dry mergers, and mixed mergers in units of number of mergers $h^3 \text{Mpc}^{-3} \text{Gyr}^{-1}$.

TABLE 2. RESULTS OF FITTING PARAMETERS FOR THE PAIR FRACTION

Pair Types	$N_c(0)^{30}$	m^{30}	$N_c(0)^{50}$	m^{50}	$N_c(0)^{100}$	m^{100}
All	0.041±0.004	0.41±0.20	0.084±0.006	0.41±0.14	0.210±0.004	0.29±0.05
Blue-Blue	0.018±0.004	1.27±0.35	0.029±0.004	1.32±0.28	0.082±0.007	1.09±0.15
Red-Red	0.045±0.009	-0.92±0.59	0.099±0.013	-0.51±0.40	0.262±0.021	-0.85±0.23
Mixed	0.029±0.005	-1.52±0.42	0.048±0.006	-0.64±0.26	0.099±0.008	-0.29±0.16

NOTE. — Here $N_c(0)$ and m are the fitting parameters for the evolution of pair fraction in the form of $N_c = N_c(0)(1+z)^m$. The superscripts 30, 50 and 100 denote the values of r_{max} in unit of $h^{-1} \text{kpc}$ used to select close pairs.

Patton, D. R., Pritchett, C. J., Yee, H. K. C., Ellingson, E., & Carlberg, R. G. 1997, *ApJ*, 475, 29
Patton, D. R., Carlberg, R. G., Marzke, R. O., Pritchett, C. J., da Costa, L. N., & Pellegrini, P. S. 2000, *ApJ*, 536, 153
Patton, D. R., et al. 2002, *ApJ*, 565, 208
Patton, D. R., & Atfield, J. E. 2008, *ApJ*, submitted.
Scarlata, C., et al. 2007, *ApJS*, 172, 494
Somerville, R. S., & Kolatt, T. S. 1999, *MNRAS*, 305, 1
Springel, V., White, S. D. M., Tormen, G., & Kauffmann, G. 2001, *MNRAS*, 328, 726
Tran, K-v. H., et al. 2005, *ApJ*, 627, L25
Toomre, A., & Toomre, J., 1972, *ApJ*, 178, 623
van Dokkum, P. G., 2005, *AJ*, 130, 2647
Weiner, B. J., et al. 2005, *ApJ*, 620, 595

Weiner, B. J., et al. 2006, *ApJ*, 653, 1027
White, M., Zheng, Z., Brown, M. J. I., Dey, A., & Jannuzi, B. T. 2007, *ApJ*, 655, L69
Willmer, C. N. A., et al. 2006, *ApJ*, 647, 853
Wirth, G. D., et al. 2004, *AJ*, 127, 3121
Woods, D., Fahlman, G. G., & Richer, H. B. 1995, *ApJ*, 454, 32
Woods, D. F., Geller, M. J., & Barton, E. J. 2006, *AJ*, 132, 197
Yee, H. K. C., & Ellingson, E. 1995, *ApJ*, 445, 37
Yee, H. K. C., Ellingson, E., & Carlberg, R. G. 1996, *ApJS*, 102, 269
Yee, H. K. C., et al. 2000, *ApJS*, 129, 475
Zepf S. E., & Koo, D. C. 1989, *ApJ*, 337, 34